RSC Advances

PAPER

View Article Online
View Journal | View Issue

Cite this: *RSC Adv.*, 2017, **7**, 44614

A water-soluble fluorescent hybrid material based on aminoclay and its bioimaging application†

Qing-Feng Li,[ab] Zengchen Liu,[ab] Lin Jin,[ab] Piaoping Yang*[c] and Zhenling Wang*[ab]

Received 3rd August 2017
Accepted 11th September 2017

DOI: 10.1039/c7ra08581h

rsc.li/rsc-advances

A water-soluble fluorescent hybrid material has been prepared by functionalization of aminoclay with a fluorescent dye (NDPA). UV-vis absorbance, FT-IR/fluorescent spectroscopy, SEM and TEM techniques were used to investigate its structural, fluorescence and morphological features. The results indicated that the organic fluorescent group can be covalently anchored onto aminoclay through the reaction of the amino-group, and the obtained AC–NDPA exhibited good water solubility and fluorescence properties, coupled with high dispersibility in aqueous solution. Further study found that AC–NDPA had low biotoxicity, and live cell imaging showed that AC–NDPA can be efficiently phagocytized by HeLa cells, bright blue emission can be observed in the cytoplasm and nucleus of HeLa cells by con-focal laser scanning microscopy. We expect that this work could reveal the potential for using the aminoclay based fluorescent material as an effective staining reagent for *in vivo* bioimaging.

Introduction

Fluorescent materials such as metal nanoclusters,[1–4] carbon or quantum dots[5–8] and lanthanide complexes[9,10] are intensively attractive for large-scale applications because of their novel and tunable properties. Among these, organic fluorescent dyes have been extensively studied owing to their potential application in fluorescence immunoassays, detection, bioimaging, *etc.*[11–14] However, in many cases these materials suffer from low solubility or dispersibility in water which greatly restricts their application in the biomedical field. Recently, some researchers reported that the hybridization of fluorescent dyes with silica and carbon materials is advantageous to improve their dispersibility in pure water, and the prepared hybrid materials have been extensively used in biomolecular sensing and cellular imaging.[15–19] However, the aggregation and precipitation of the resulting dispersion should be considered in fluorescence qualitative or quantitative detection.

Aminoclay (AC) reported by Mann and co-workers is a water soluble, amino-containing organic clay with a talc-like structure.[20] The feature about AC is its reversible exfoliation by electrostatic repulsion of protonated amino-groups, which makes it easier to dissolve in pure water under neutral pH.[21–23] At present, several AC based fluorescent composites have been prepared by non-covalent electrostatic self-assembly between protonated AC and organic dyes.[24–26] As a strong nucleophile, amino-group can also provide great potential for covalent modification of AC *via* nucleophilic substitution, Michael-like addition and amidation reaction.[27–29] Hence, it is reasonable to envisage the covalent linkage of organic dyes to AC through the reaction of amino-group to obtain the water-soluble fluorescent materials. We believe that this method can be one of the effective strategies for the synthesis of water soluble hybrid fluorescent materials by means of molecular design technology.

It is well known that fluorescence imaging technique is a powerful tool for observing bio-molecular interactions. In general, the staining materials used in bio-imaging should have a low biotoxicity and good fluorescent property, coupled with high dispersibility in water so that they can be phagocytized by living cells. According to the above analysis, we prepared a water-soluble fluorescent material (AC–NDPA) by the amino-acylation reaction between NDPA and AC, in which AC plays the role of solubilization. SEM and TEM analysis showed that AC–NDPA can be exfoliated into many nano-sized pieces by electrostatic repulsion of protonated amino-groups. *In vivo* assessments using L929 fibroblast cells revealed that AC–NDPA had low cytotoxicity and live cell imaging demonstrated that it has great potential of stain capability in HeLa cells.

Results and discussion

The synthesis procedures of NDPA and AC–NDPA were illustrated in Scheme 1. NDPA was synthesized by nucleophilic

[a]*The Key Laboratory of Rare Earth Functional Materials and Applications, Zhoukou Normal University, Zhoukou 466001, Henan, P. R. China. E-mail: zlwang2007@hotmail.com; Fax: +86-394-8178518; Tel: +86-394-8178518*

[b]*International Joint Research Laboratory for Biomedical Nanomaterials of Henan, Zhoukou Normal University, Zhoukou 466001, P. R. China*

[c]*Key Laboratory of Superlight Materials and Surface Technology, Ministry of Education, College of Material Science and Chemical Engineering, Harbin Engineering University, Harbin 150001, P. R. China. E-mail: yangpiaoping@hrbeu.edu.cn*

† Electronic supplementary information (ESI) available: NMR, XRD, FL spectra, and luminescence decay curves. See DOI: 10.1039/c7ra08581h

substitution reaction of bis(2-pyridylmethyl)amine with naphthalimide in 2-methoxyethanol, and characterized by ^{1}H-NMR, ^{13}C-NMR and mass spectroscopy, respectively (Fig. S1 and S2†). AC–NDPA was prepared through the amidation reaction between cyclic anhydride of NDPA and the amino-group of AC. It should be pointed out that the presence of water molecular can result in the protonation of amino-group, and the electrostatic repulsion between the protonation of amino-group will easily cause the dissolution of AC in water.

FT-IR spectra were utilized to prove the successful covalent attachment of NDPA to AC. As shown in Fig. 1, the pure AC showed the typical vibration bands of the layered magnesium organosilicates, such as the stretching vibrations of Mg–O at 566 cm^{-1}, stretching of C–H at 2815 cm^{-1}, asymmetric stretching of Si–O–Si and C–H at 1035 cm^{-1} and 2934 cm^{-1}, respectively (Fig. 1a).[20] In addition, the IR spectrum of NDPA showed two obvious peaks at 1756 and 1722 cm^{-1} due to the vibrational coupling of carbonyl groups in cyclic anhydride (Fig. 1b). However, after being modified by AC, these two peaks were shifted to 1689 and 1643 cm^{-1},[30] indicated that the cyclic anhydride of NDPA was reacted with the amino-group of AC to generate the new amide carbonyl group. Moreover, several new peaks appeared in the spectrum (Fig. 1c) compared with that of AC, the peaks at 1585 and 1481 cm^{-1} which could be ascribed to the skeleton stretching vibration of aromatic ring, also showed the successful ligation of AC and NDPA.

UV-vis absorption spectra of AC, AC–NDPA and NDPA are shown in Fig. 2. As expected, no discernible absorption peak was found in the UV or visible region for pure AC (Fig. 2a). However, as shown in Fig. 2b, two distinct broad absorption bands around 260 nm and 415 nm are observed, which indicates the presence of organic conjugated moiety in the modified AC.[31] Moreover, the absorption spectrum of AC–NDPA shows a clear red shift in the visible region compared with that of NDPA (Fig. 2c). In fact, the amidation reaction results in an increase conjugation effect in aromatic system which causes a red-shift of the UV-vis absorption spectrum.

AC–NDPA can be dissolved in water to form a yellowish transparent solution, which shows strong visible yellow-green fluorescence under UV light excitation (365 nm) (inset of Fig. 3). Furthermore, the optical properties of AC–NDPA were investigated by fluorescence spectrum. The excitation spectrum of AC–NDPA solution monitored at 503 nm possesses a broad excitation band, which can be attributed to the $\pi \rightarrow \pi^*$ electronic transition of organic moiety in AC–NDPA (Fig. S3†). Meanwhile, an obvious fluorescence emission band between 400 and 700 nm (λ_{max} = 503 nm) was observed when AC–NDPA solution was excited by the UV light of 330 nm (Fig. 3). The fluorescence lifetime value of AC–NDPA solution was determined by the corresponding decay curves that can be well fitted into a double-exponential function, and the average lifetime was determined to be 2.54 ns (Fig. S4†). Moreover, the effect of pH value, time and NaCl concentration on the fluorescence intensity of AC–NDPA solution was investigated. As shown in Fig. S5,† the fluorescence intensity of AC–NDPA solution has not changed much with varying concentration of NaCl, time (within 24 h) and pH from 7 to 10, indicating that AC–NDPA has good luminescence stability in aqueous solution.

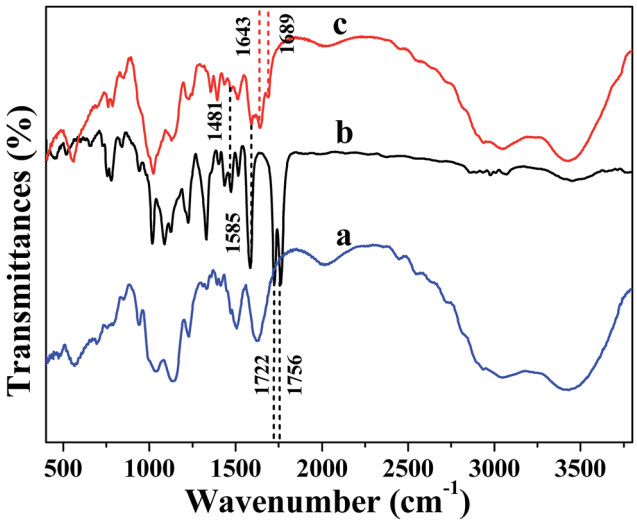

Fig. 1 FT-IR spectra of AC (a), NDPA (b) and AC–NDPA (c).

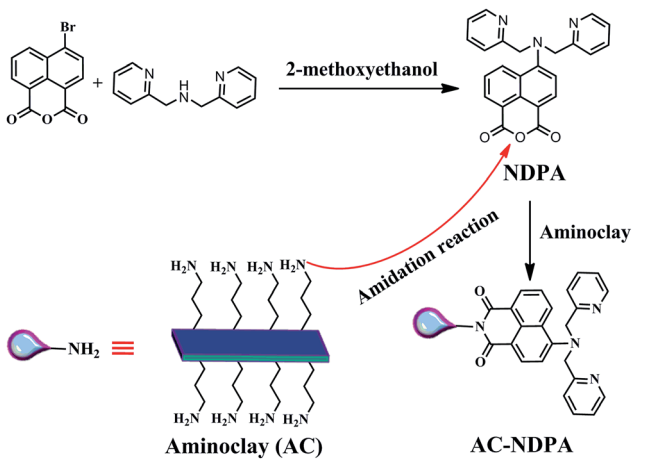

Scheme 1 Synthesis procedures of AC–NDPA.

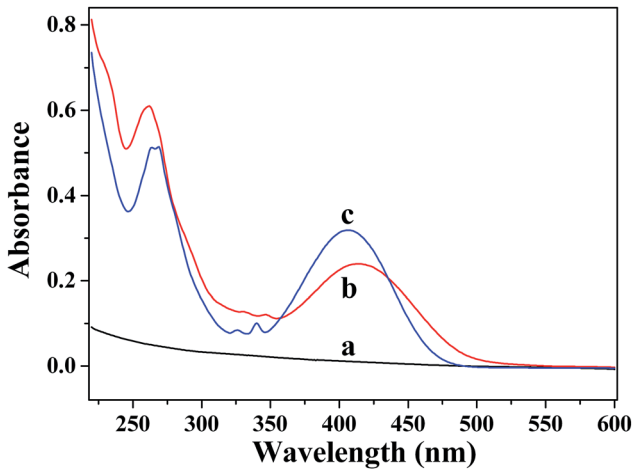

Fig. 2 UV-vis absorption spectra of AC (a), AC–NDPA (0.25 mg mL^{-1}) (b) and NDPA (0.02 mg mL^{-1}) (c).

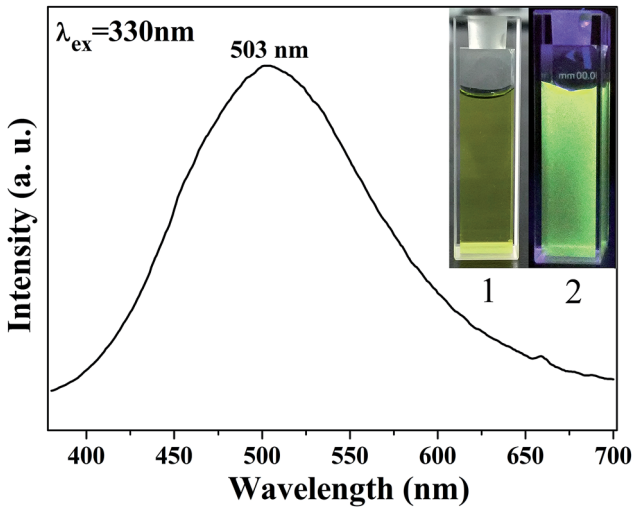

Fig. 3 Fluorescence spectrum of AC–NDPA solution with the excitation of 330 nm (1 mg mL^{-1}), insets of figure is the digital photos of AC–NDPA solution taken under daylight (1) and UV light of 365 nm (2).

The structural features of pure AC and modified AC were investigated by X-ray diffraction measurements (Fig. S6†). The interlayer spacing of d_{001} was determined to be 1.6 nm according to the Bragg's law, corresponding to the bilayer arrangement of aminopropyl groups. And three higher angle reflections at $2\theta = 23°$, 36°, 59° confirm the formation of the disordered, talc-like structure analogous to 2 : 1 trioctahedral phyllosilicate clay.[32] Moreover, the exfoliation behavior of AC–NDPA in water was confirmed by using SEM and TEM observation. As shown in Fig. 4a and b, the agminated AC–NDPA exhibits a stacked lamellar structure with the characteristic clay sheet edges. However, it is found that AC–NDPA can be exfoliated into many small pieces

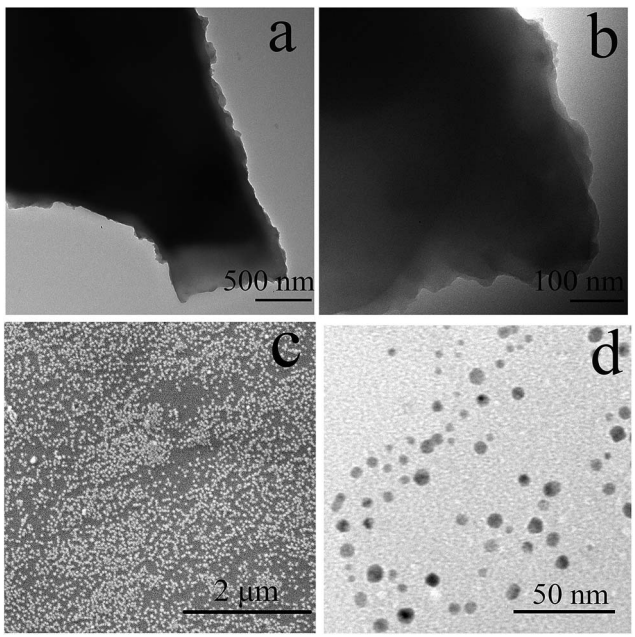

Fig. 4 TEM images of AC–NDPA dispersed in acetone (a, b), SEM (c) and TEM (d) of AC–NDPA dispersed in water.

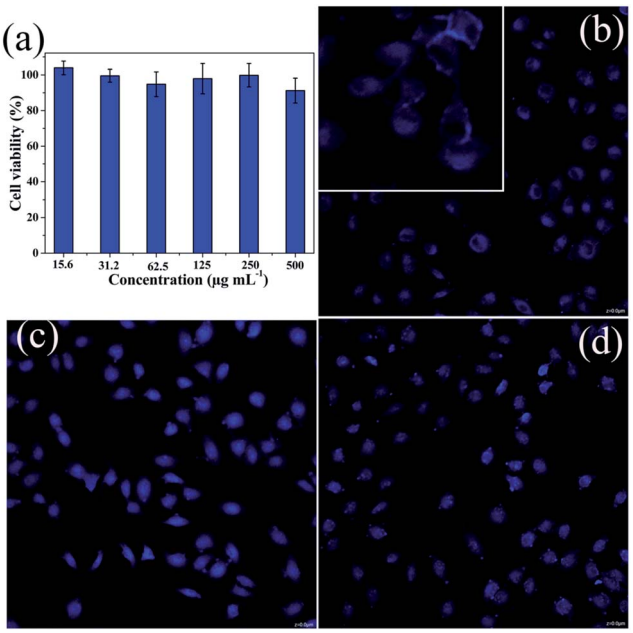

Fig. 5 Cell viability for L929 fibroblast cells incubated with AC–NDPA with different concentrations for 24 h (a), con-focal laser scanning microscopy images of HeLa cells incubated with AC–NDPA for 0.5 h (b), 1 h (c), 3 h (d).

with an diameter of about 20 nm by protonated amine groups (Fig. 4c and d), which makes it very soluble in water.[32–34]

Furthermore, taking into account its small particle size and good dispersity in aqueous solution, AC–NDPA may be a promising material for biological applications. To further evaluate the feasibility of bio-imaging in living cells, the biocompatibility should be first investigated. Herein, cell viability for L929 fibroblast cells incubated with different concentrations of AC–NDPA was tested with the MTT assay.[35,36] As shown in Fig. 5a, AC–NDPA shows no obvious toxic effect on the normal cells, even at a relative high concentration up to 500 μg mL^{-1}, indicating the good biocompatibility in living cells.[37,38] Therefore, we used con-focal laser scanning microscopy (CLSM) to observe the cellular uptake of AC–NDPA, and the cell uptake process was verified by the CLSM photographs of HeLa cells incubated with AC–NDPA for 0.5 h, 1 h, and 3 h at 37 °C in the dark. After incubation for 0.5 h, weak blue emission was observed around the cell membrane because only a few AC–NDPA have been phagocytized by HeLa cells (Fig. 5b). With increase of the incubation time, bright blue emission was observed throughout the cells, suggesting that a considerable amount of AC–NDPA was exchanged into the cytoplasm and nucleus of HeLa cells (Fig. 5c and d). This result reveals that the AC–NDPA can be effectively taken up by HeLa cells, which will make it a suitable material for bio-imaging and biological applications.

Experimental section

Synthesis of aminoclay

The typical synthesis process of aminoclay followed the previous procedure.[39,40] $MgCl_2 \cdot 6H_2O$ (0.84 g) was dissolved into

20.0 mL absolute alcohol, and 3-aminopropyltriethoxysilane (1.3 mL) was dropwisely added to the above solution. The obtained white emulsion was stirred for about 24 h at room temperature. The white precipitate was collected by centrifugation, washed with absolute alcohol, and dried under vacuum at 60 °C for 8 h.

Synthesis of NDPA

4-Bromo-1,8-naphthalic anhydride (0.30 g), di-(2-picolyl)amine (0.30 g) were added to 2-methoxyethanol (25 mL), and the resulting solution was refluxed for 48 h under an atmosphere of nitrogen. Then the solvent was removed by evaporation, and the residue was purified by column chromatography (silica gel, ethyl acetate : dichloromethane = 1 : 1) to yield a yellow solid (0.28 g, 65%). ^{1}H-NMR (300 MHz, DMSO-d_6) δ ppm: 9.00 (d, 1H), 8.54 (d, 2H), 8.48 (d, 1H), 8.26 (d, 1H), 7.82 (t, 1H), 7.74 (m, 2H), 7.46 (d, 2H), 7.27 (m, 3H), 4.77 (s, 4H). ^{13}C-NMR (300/4 MHz, DMSO-d_6) δ ppm: 161.7, 160.7, 157.5, 155.4, 149.8, 137.4, 133.9, 133.0, 132.5, 132.4, 126.5, 126.1, 123.1, 122.8, 119.8, 117.2, 111.0, 59.4. ESI-MS: m/z calcd for $C_{24}H_{17}N_3O_3$: 396.4180 $[M+1]^+$, found: 396.1347.

Synthesis of AC–NDPA

Aminoclay (AC, 0.5 g) and 6-(bis(pyridin-2-ylmethyl)amino) benzo[*de*]isochromene-1,3-dione (NDPA, 80 mg) were added to dry toluene (20 mL). The resulting mixture was refluxed at 110 °C for 24 h under an atmosphere of nitrogen. The suspension was centrifuged and the solid residue was washed with CH_2Cl_2. After dried under vacuum at 60 °C for 8 h, the hybrid fluorescent material AC–NDPA was obtained. The weight of the recovered NDPA was 30.7 mg, thus, about 62% of NDPA was successfully grafted onto the aminoclay.

Cell viability test

First, L929 fibroblast cells where were obtained from the cell bank of the Chinese Academy of Sciences (Shanghai, China) were cultivated in a 96-well plate and cultured for 24 h with CO_2 (5%) at 37 °C, and AC–NDPA solution (15.6, 31.2, 62.5, 125, 250, 500 μg mL^{-1}) were added to the wells and incubated for 24 h at 37 °C in 5% CO_2. One set of blank control (6 wells) was left with culture only. Next, 0.02 mL of MTT solution was added to each well and the cells were incubated for another 4 h at the same condition. Finally, DMSO (0.15 mL) was added into each well and the plate was shaken for 10 min to blend the solvent and formazan crystals completely. The optical absorbance of each well at 490 nm was recorded using a micro-plate reader. The cell viability was determined by the following equation:

$$\text{Cell viability (\%)} = (\text{absorbance of test cells/absorbance of blank controlled cells}) \times 100\%.$$

Cellular uptake

The cellular uptake of AC–NDPA by HeLa cells was examined using a confocal laser scanning microscope (CLSM, Leica SP8). HeLa cells (5×10^4 per well) were plated in 6-well culture plate and grown for 24 h at 37 °C before uptake study. And then the HeLa cells were incubated with AC–NDPA (2 mL, 500 μg mL^{-1}) at 37 °C for different times (0.5, 1, 3 h), followed by rinsing with PBS buffer three times. Subsequently, the harvested cells were fixed with formaldehyde (2.5%, 1 mL per well) at 37 °C for 10 min and rinsed with PBS buffer three times.

Characterization

XRD analysis of AC and AC–NDPA was carried out using a Bruker D8 advance X-ray diffractometer. UV-vis absorbance spectra were obtained on a Perkin-Elmer Lambda 35 spectrophotometer. FT-IR spectra were recorded with a Thermo Nicolet 5700 spectrophotometer (KBr pellet). Transmission electron microscopy (TEM) analysis was performed by a Hitachi HT 7700 electron microscope operating at an accelerating voltage of 100 kV. Scanning electron microscopy (SEM) image was obtained with a FEI Quanta 200 electron microscope. The fluorescence spectra and lifetimes were measured using an Edinburgh FLS920P spectrometer under neutral pH conditions. ^{1}H-NMR and ^{13}C-NMR spectra were acquired on a Bruker AV300 NMR spectrometer at 300 MHz.

Conclusions

In summary, we developed a synthesis strategy for preparation of water-soluble hybridization fluorescence material by covalently grafting organic fluorescent group to aminoclay. The obtained AC–NDPA can be exfoliated into nano-sized pieces in water, and its aqueous solution exhibits good fluorescence emission. Moreover, AC–NDPA could be used as a staining reagent in living cells due to its good biocompatibility. We expect that the biocompatible hybrid material will promote fluorescent dyes application for *in vivo* biological studies.[41,42]

Conflicts of interest

There are no conflicts to declare.

Acknowledgements

This work is financially supported by the National Natural Science Foundation of China (no. 21401218, 51572303, 21701203), the Innovation Scientists and Technicians Troop Construction Projects of Henan Province (2013259), the Program for Innovative Research Team (in Science and Technology) in University of Henan Province (no. 14IRTSTHN009), the Key Scientific and Technological Project of Henan Province (172102410024), and the Program of Innovative Talent (in Science and Technology) in the University of Henan Province (17HASTIT007).

Notes and references

1 K. Y. Zheng, M. I. Setyawati, D. T. Leong and J. P. Xie, *ACS Nano*, 2017, **11**, 6904–6910.
2 N. Goswami, Q. F. Yao, Z. T. Luo, J. G. Li, T. K. Chen and J. P. Xie, *J. Phys. Chem. Lett.*, 2016, **7**, 962–975.

3 K. Y. Zheng, M. I. Setyawati, T. P. Lim, D. T. Leong and J. P. Xie, *ACS Nano*, 2016, **10**, 7934–7942.
4 J. S. Martinez and J. P. Xie, *APL Mater.*, 2017, **5**, 053001.
5 Y. B. Song, S. J. Zhu and B. Yang, *RSC Adv.*, 2014, **4**, 27184–27200.
6 Y. F. Zhao, L. Y. Shi, J. H. Fang and X. Feng, *Nanoscale*, 2015, **7**, 20033–20041.
7 S. F. Wuister, I. Swart, F. van Driel, S. G. Hickey and C. d. M. Donegá, *Nano Lett.*, 2003, **3**, 503–507.
8 Y. Li, Z. M. Liu, Y. Q. Hou, G. C. Yang, X. X. Fei, H. N. Zhao, Y. X. Guo, C. K. Su, Z. Wang, H. Q. Zhong, Z. F. Zhuang and Z. Y. Guo, *ACS Appl. Mater. Interfaces*, 2017, **9**, 25098–25106.
9 Q. F. Li, D. Yue, G. W. Ge, X. D. Du, Y. C. Gong, Z. L. Wang and J. H. Hao, *Dalton Trans.*, 2015, **44**, 16810–16817.
10 Q. F. Li, X. D. Du, L. Jin, M. M. Hou, Z. L. Wang and J. H. Hao, *J. Mater. Chem. C*, 2016, **4**, 3195–3201.
11 Y. Zhou and J. Yoon, *Chem. Soc. Rev.*, 2012, **41**, 52–67.
12 H. Kwon, K. Lee and H. J. Kim, *Chem. Commun.*, 2011, **47**, 1773–1775.
13 A. Keppler, H. Pick, C. Arrivoli, H. Vogle and K. Johnsson, *Proc. Natl. Acad. Sci. U. S. A.*, 2004, **101**, 9955–9959.
14 Y. Zhao, B. Z. Zheng, J. Du, D. Xiao and L. Yang, *Talanta*, 2011, **85**, 2195–2201.
15 T. H. Kim, D. Lee and J. W. Choi, *Biosens. Bioelectron.*, 2017, **94**, 485–499.
16 N. Lashgari, A. Badiei, G. M. Ziarani and F. Faridbod, *Anal. Bioanal. Chem.*, 2017, **409**, 3175–3185.
17 S. K. Rastogi, P. Pal, D. E. Aston, T. E. Bitterwolf and A. L. Branen, *ACS Appl. Mater. Interfaces*, 2011, **3**, 1731–1739.
18 Z. B. Sun, H. Z. Li, D. Guo, J. Sun, G. J. Cui, Y. Liu, Y. X. Tian and S. Q. Yan, *J. Mater. Chem. C*, 2015, **3**, 4713–4722.
19 Z. P. Dong, B. Yang, J. Jin, J. Li, H. W. Kang, X. Zhong, R. Li and J. T. Ma, *Nanoscale Res. Lett.*, 2009, **4**, 335–340.
20 S. L. Burkett, A. Press and S. Mann, *Chem. Mater.*, 1997, **9**, 1071–1073.
21 K. K. R. Datta, A. Achari and M. Eswaramoorthy, *J. Mater. Chem. A*, 2013, **1**, 6707–6718.
22 K. K. R. Datta, M. Eswaramoorthy and C. N. R. Rao, *J. Mater. Chem.*, 2007, **17**, 613–615.
23 S. H. Wang, H. Cao and Y. M. Zhong, *J. Mater. Chem. B*, 2016, **4**, 4295–4301.
24 K. V. Rao, K. K. R. Datta, M. Eswaramoorthy and S. J. George, *Angew. Chem., Int. Ed.*, 2011, **50**, 1179–1184.
25 T. R. Wang, M. Q. Liu, Q. Ji and Y. G. Wang, *RSC Adv.*, 2015, **5**, 103433–103438.
26 K. V. Rao, K. K. R. Datta, M. Eswaramoorthy and S. J. George, *Adv. Mater.*, 2013, **25**, 1713–1718.
27 L. H. Zhi, Z. Y. Wang, J. Liu, W. S. Liu, H. L. Zhang, F. J. Chen and B. D. Wang, *Nanoscale*, 2015, **7**, 11712–11719.
28 Y. Liu, L. N. Sun, J. L. Liu, Y. X. Peng, X. Q. Ge, L. Y. Shi and W. Huang, *Dalton Trans.*, 2015, **44**, 237–246.
29 Q. F. Li, L. Jin, L. L. Li, W. P. Ma, Z. L. Wang and J. H. Hao, *J. Mater. Chem. C*, 2017, **5**, 4670–4676.
30 C. S. Zhao, X. L. Liu, M. Yang, J. Y. Fang, J. J. Zhang and F. Q. Liu, *Dyes Pigm.*, 2009, **82**, 134–141.
31 J. F. Zhang, M. Park, W. X. Ren, Y. Kim, S. J. Kim, J. H. Jung and J. S. Kim, *Chem. Commun.*, 2011, **47**, 3568–3570.
32 S. Ravula, J. B. Essner, W. A. La, L. Polo-Parada, R. Kargupta, G. J. Hull, S. Sengupta and G. A. Baker, *Nanoscale*, 2015, **7**, 86–91.
33 A. J. Patil, E. Muthusamy and S. Mann, *Angew. Chem., Int. Ed.*, 2004, **43**, 4928–4933.
34 Y. C. Lee, W. K. Park and J. W. Yang, *J. Hazard. Mater.*, 2011, **190**, 652–658.
35 D. Yang, G. X. Yang, X. M. Wang, R. C. Lv, S. L. Gai, F. He, A. Gulzar and P. P. Yang, *Nanoscale*, 2015, **7**, 12180–12191.
36 J. T. Xu, Y. Kuang, R. C. Lv, P. P. Yang, C. X. Li, H. T. Bi, B. Liu, D. Yang, Y. L. Dai, S. L. Gai, F. He, B. G. Xing and J. Lin, *Biomaterials*, 2017, **130**, 42–55.
37 Y. Zhuo, H. Miao, D. Zhong, S. S. Zhu and X. M. Yang, *Mater. Lett.*, 2015, **139**, 197–200.
38 J. Vinayagam, G. R. Chen, T. Y. Huang, J. H. Ho, Y. C. Ling, K. L. Ou and J. Y. Chang, *Mater. Lett.*, 2016, **173**, 242–247.
39 Y. Hwang, Y. C. Lee, P. D. Mines, Y. K. Oh, J. S. Choi and H. R. Andersen, *Chem. Eng. Sci.*, 2014, **119**, 310–317.
40 S. J. Hoseini, M. Rashidi and M. Bahrami, *J. Mater. Chem.*, 2011, **21**, 16170–16176.
41 A. B. Descalzo, M. D. Marcos, R. Martínez-Máñez, J. Soto, D. Beltránb and P. Amorósb, *J. Mater. Chem.*, 2005, **15**, 2721–2731.
42 Z. B. Sun, D. Guo, H. Z. Li, L. Zhang, B. Yang and S. Q. Yan, *RSC Adv.*, 2015, **5**, 11000–11008.

